Expression of alternative NADH dehydrogenases (NDH-2) in the phytopathogenic fungus *Ustilago maydis*

Deyamira Matuz-Mares[1], Genaro Matus-Ortega[2], Christian Cárdenas-Monroy[1],
Lucero Romero-Aguilar[3], Juan Carlos Villalobos-Rocha[1], Héctor Vázquez-Meza[1],
Guadalupe Guerra-Sánchez[3], Antonio Peña-Díaz[2] and Juan Pablo Pardo[1]

1 Departamento de Bioquímica, Facultad de Medicina, Universidad Nacional Autónoma de México, Ciudad de México, México
2 Departamento de Genética Molecular, Instituto de Fisiología Celular, Universidad Nacional Autónoma de México, Ciudad de México, México
3 Bioquímica de hongos, Escuela Nacional de Ciencias Biológicas, Instituto Politécnico Nacional, Ciudad de México, México

Type 2 alternative NADH dehydrogenases (NDH-2) participate indirectly in the generation of the electrochemical proton gradient by transferring electrons from NADH and NADPH into the ubiquinone pool. Due to their structural simplicity, alternative NADH dehydrogenases have been proposed as useful tools for gene therapy of cells with defects in the respiratory complex I. In this work, we report the presence of three open reading frames, which correspond to NDH-2 genes in the genome of *Ustilago maydis*. These three genes were constitutively transcribed in cells cultured in YPD and minimal medium with glucose, ethanol, or lactate as carbon sources. Proteomic analysis showed that only two of the three NDH-2 were associated with isolated mitochondria in all culture media. Oxygen consumption by permeabilized cells using NADH or NADPH was different for each condition, opening the possibility of posttranslational regulation. We confirmed the presence of both external and internal NADH dehydrogenases, as well as an external NADPH dehydrogenase insensitive to calcium. Higher oxygen consumption rates were observed during the exponential growth phase, suggesting that the activity of NADH and NADPH dehydrogenases is coupled to the dynamics of cell growth.

Type 2 NADH dehydrogenases (NDH-2) are alternative respiratory components that allow a cellular response to different environmental conditions [1]. NDH-2 have molecular masses of about 50–60 kDa, and they are typically attached to both sides of the inner mitochondrial membrane. These proteins are insensitive to rotenone but sensitive to flavone [2,3]. As NDH-2 do not pump protons (H^+) across the membrane, they have no direct participation in the generation of the proton electrochemical gradient [4,5]; however, NDH-2 allow the transfer of electrons from NADH and NADPH into the respiratory chain, supporting the synthesis of ATP [6,7].

The presence of alternative components such as NDH-2 in the electron transport chain was first

Abbreviations

6PGD, 6 phosphogluconate dehydrogenase; Aox, alternative oxidase; EtOH-DH, ethanol dehydrogenase; EtOH-mm, ethanol minimal medium; Fum, fumarate; G3P-DH, glycerol 3-phosphate dehydrogenase; G6P-DH, glucose 6-phosphate dehydrogenase; Glc-mm, glucose minimal medium; HK, hexokinase; HK, hexokinase; Lac-DH, lactate dehydrogenase; Lac-mm, lactate minimal medium; Mal, malate; NDH-2, alternative NADH dehydrogenases; OAA, oxaloacetate; PFK-1, phosphofructokinase 1; PK, pyruvate kinase; Pyr, pyruvate; Succ, succinate; YPD, yeast extract, peptone, and dextrose medium.

described in mitochondria of plants and fungi, and later, they were found in the plasma membrane of several Eubacteria and Archaea [8]. Transcripts of these alternative elements were also present in animals from marine environments [9]. The 3-D structure of the *Saccharomyces cerevisiae* internal NADH dehydrogenase (scNdi1) corresponds to a homodimeric protein, with a hydrophobic region that allows its binding to the membrane [10,11]. A similar structure was described for *Caldalkalibacillus thermarum*'s NDH-2 [12]. Besides scNdi1, *S. cerevisiae* has two additional alternative components: the external NADH dehydrogenases scNde1 and scNde2 [13,14]. It has been shown that scNdi1 is part of respiratory supercomplexes [15,16], similar to the respirasomes described in mitochondria of plant, fungi, and animal cells [17–19]. An understanding of NDH-2 is of great importance because they are potential targets of pharmacological agents against parasites of animals and plants that became resistant to traditional antibiotics [20–22]. On the other hand, scNdi1 has also been proposed for gene therapy to rescue cells with defects in complex I [23–25] .

In *Ustilago maydis*, a phytopathogenic fungus of *Zea mays* which establishes a biotrophic relationship with the plant, the presence of at least one external and one internal NDH-2 has been described, as well as an alternative oxidase (Aox) [26].

Through an *in silico* analysis, three open reading frames for NDH-2 were found in *U. maydis* genome. The three predicted amino acid sequences (um02164, um03669, and um11333) contained two Rossman fold domains and two glycine-rich motifs for the binding of NAD(P)H and FAD. One of these enzymes (um03669) shows a putative calcium binding domain. To evaluate the activity of NDH-2s in *U. maydis*, oxygen consumption assays were performed in permeabilized cells cultured under glycolytic (glucose) or gluconeogenic (ethanol and lactate) growth conditions [27]. The results showed the presence of rotenone-insensitive NADH dehydrogenase activity on both sides of the inner mitochondrial membrane and an external NADPH dehydrogenase activity. Under all conditions, NDH-2 activities were higher at the exponential phase than in the stationary phase of the growth curve. There was no activation by calcium of the alternative NADPH dehydrogenase under any condition. Transcripts of the three genes were expressed in all culture conditions, but only two of the three NDH-2 proteins (um03669 and um02164) were found in mitochondria. Oxygen consumption rates with NADH or NADPH were different in the two growth phases of the cells.

Materials and methods

Materials

Analytical grade reagents were purchased from Sigma Chemical Co. (St. Louis, MO, USA), Bio-Rad (Hercules, CA, USA), Agilent Technologies (La Jolla, CA, USA), Axygen Biosciences (Union City, CA, USA), and Millipore (Billerica, MA, USA). *Ustilago maydis* ATCC 201384 FB2 was obtained from the American Type Cell Collection (Manassas, VA, USA).

Bioinformatic methods

To obtain the NDH-2 sequences of *U. maydis,* a protein BLAST [28] in the *U. maydis* database (https://www.helmholtz-muenchen.de/ibis/institute/groups/fungal-microbial-genomics/resources/mumdb/index.html) was performed. Multiple sequence alignment of the NDH-2 amino acid sequences was carried out with Clustal X [29]. Pairwise identities were calculated by local sequence alignment, using SIM (http://ca.expasy.org/tools/sim-prot.html), with a gap open penalty of 12, a gap extension penalty of 4, and BLOSUM62 as the comparison matrix. MITOPROT was used for the prediction of mitochondrial signal peptides [30].

Strains and cell cultures

Ustilago maydis strains were grown at 28 °C in either rich YPD medium (1.0% glucose, 0.25% peptone, and 0.5% yeast extract) or minimal medium (mm) supplemented with different carbon sources (1.0% glucose, 0.4% ethanol, or 1.0% lactate), and 0.3% ammonium sulfate as the nitrogen source, and supplemented with 1x salt solution [31]. In all cases, cells were cultured in 100 mL of YPD medium for 18–24 h, harvested by centrifugation at 1000 g, and washed twice with sterile H_2O, and the final suspension was used to inoculate 1 L of medium with 4.5×10^8 cells (initial OD of 0.02 at 600 nm). Cells were harvested at the exponential or stationary phases of growth and suspended in distilled H_2O at a final ratio of 1 mL·g^{-1} wet weight. Cell growth was followed by measuring the optical density at 600 nm.

Cell permeabilization and oxygen consumption

Plasma membrane permeabilization was achieved by incubation of *U. maydis* cells with 0.03% of digitonin for approximately 1 min inside the Clark electrode chamber, as described by Vercesi [27] and Robles-Martínez [32]. All experiments were carried out in KME buffer (100 mM KCl, 50 mM Mops/KOH, and 0.5 mM EGTA, pH 7.4). Oxygen consumption was measured in a 1.5 mL chamber at 30 °C, using a Clark-type electrode connected to an YSI5300A biological oxygen monitor. The assays were carried out using 5 to 10 mg of cells (wet weight), and after the

experiment, an aliquot of the cell suspension was used to obtain the dry weight. NADH, NADPH, pyruvate–malate, succinate, ethanol, glycerol-3-phosphate, and lactate were used as substrates.

Mitochondria isolation

The method described by Sierra-Campos [33] was used with minor modifications: Cells were collected by centrifugation at 5000 g for 5 min, 4 °C and washed twice with lysis buffer (20 mM Tris/HCl, 330 mM sucrose, 2 mM EDTA, 1 mM EGTA, 100 mM KH_2PO_4) and the final pellets resuspended in 1 mL of the lysis supplemented with 0.2% BSA, 0.5 mM β-mercaptoethanol, and 1 mM PMSF. Rupture of the cells was performed at 4 °C by a mechanical method, using a Mini-Bead Beater with glass beads of 0.5 μm of diameter. To avoid damage of mitochondria, four cycles of 30 s were selected for the rupture, with 2 min pauses on ice. The crude extract was centrifuged at 5000 g for 10 min at 4 °C. The supernatant was recovered and centrifuged at 10 000 g for 10 min at 4 °C, and the mitochondrial pellet was suspended in a small volume of lysis buffer and kept at −70 °C.

Enzyme assays

The activities of glycolytic enzymes were determined as described by Saavedra *et al.* [34].

Determination of protein concentration

Protein concentration was determined as described by Lowry *et al.*, using bovine serum albumin (BSA) as standard.

Sodium dodecyl sulfate polyacrylamide gel electrophoresis

Mitochondrial proteins were resolved by SDS/PAGE on 10% (w/v) polyacrylamide slab gels [35].

Tandem mass spectrometry (LC/ESI-MS/MS)

Mitochondrial samples were subjected to electrophoresis, and both the whole lane and a piece of the gel containing bands between 30 and 90 kDa were sent to the Proteomics Core Facility at the University of Arizona, USA, where the proteins associated with mitochondria were identified with 99.9% confidence.

RNA extraction and RT-PCR

To measure the RNA expression of um11333, um02164, and um03669, cells grown under the different culture conditions were harvested at the stationary phase (24 h for Glc, YPD, and EtOH, and 150 hrs for lactate), followed by RNA purification using the AxyPrep Multisource Total RNA Miniprep Kit (Axygen Biosciences). One microgram of total RNA was reverse transcribed using the protocol for gene-specific of the iScriptTM Select cDNA Synthesis Kit. The *U. maydis* actin gene was used as endogenous control. Primers used for the cDNA synthesis and RT-PCR are shown in Table 1.

Statistical analysis

To evaluate the significance of the differences between the distinct groups, a one-way or two-way ANOVA were applied to the data. The one-way ANOVA was used when growth conditions (YPD, Glc-mm, Lac-mm, and EtOH-mm) were tested against each respiratory substrate. The two-way ANOVA considered two factors, growth conditions and expression of each mRNA for the PCR experiment, and growth conditions and growth phase for the activity of each respiratory substrate.

Results and Discussion

In a previous work, some of the components of the respiratory chain of *U. maydis* mitochondria were identified using permeabilized cells [33,36]. The activity of both rotenone-insensitive external and internal NADH dehydrogenase was described. In addition, low activities associated with both glycerol 3-phosphate and NADPH dehydrogenases were found. Activities for lactate or alcohol dehydrogenase were not detected. Here, we analyzed the expression of some of these enzymes in cells grown under different conditions and at different stages of the growth curve.

Bioinformatic analyses

To determine the number of NDH-2 genes present in the *U. maydis* genome, a basic local alignment search (BLAST) was performed (https://blast.ncbi.nlm.nih.gov). The amino acid sequence of the internal NADH dehydrogenase (scNdi1) of *S. cerevisiae* was used as a query. We found three putative open reading frames for NDH-2, *UM02164*, *UM3669*, and *UM1133*. We found that the protein with the highest similarity to scNdi1 was um02164, with a value of 51%, and an identity of 34%; the other two amino acid sequences showed identities higher than 25% and similarities above 40%. MITOPROT (http://ihg.gsf.de/ihg/mitoprot.html) analysis of these three sequences showed the presence of mitochondrial signal peptides in each protein. The probability of exporting to mitochondria

Table 1. Primers used for the cDNA synthesis and the amplification of each *U. maydis* NDH-2 transcript. After the extraction of total RNA from cells, cDNA was synthetized with the cDNA primers, following the protocol for gene-specific described in iScriptTM Select cDNA Synthesis Kit®. Next, the forward and reverse primers were used to amplify short regions (200 bp) of each cDNA.

Primers	cDNA	Forward DNA	Reverse DNA
um11333	5'-AGGACGAGTCCAACAAGGAC-3'	5'-AGGACGAGTCCAACAAGGAC-3'	5'-GACCCTGGTGTGTGTACTGG-3'
um02164	5'-TTATCTCGCCGCACAACTAC-3'	5'-TTATCTCGCCGCACAACTAC-3'	5'-TCGCTCCTATCCTCGAAAGT-3'
um03669	5'-CTAGGCAGCATGTACGCACT-3'	5'-CTAGGCAGCATGTACGCACT-3'	5'-CGTCGTACTGGTCAAACACC-3'
Actin	5'-TTAGAAGCACTTGCGGTGCACG-3'	5'-GACTTGGACATCCGAAAGGA-3	5'-TTCGAGATCCACATCTGCTG-3'

was 0.8972, 0.9896, and 0.9940 for um11333, um02164, and um03669, respectively. The alignment of 12 NDH-2 sequences from fungi and one from plants (*Solanum tuberosum* NDB1soltu) revealed the high conservation of the two nucleotide binding motifs (Fig. 1A,B). The amino acid residues required for the binding of NADH and NADPH are highlighted in Fig. 2. In both um02164 and um11333 sequences, the classic acidic motif (EA) is present, and these enzymes might have NADH dehydrogenase activity, while um03669 has nonacidic amino acid residues (QS), suggesting that only this isoform might have both NADH and NADPH dehydrogenase activities as suggested by Desplats [37], Blaza [38], and Meng-Shu [39].

The protein um03669 is grouped in the NDH-2 B clade [5,40], contains a putative calcium binding domain (CBD) (Fig. 2) with similarity to the CBD of other fungal (*Kluyveromyces lactis* and *Neurospora crassa*, klNDE2 and nceNd1), and plant (*Solanum tuberosum*, NDB1_SOLTU) NDH-2s, where activation by calcium has been proposed [41–44]. However, activation by calcium was not detected in klNDE2 [45]. Another case in which the presence of a putative calcium binding domain was not associated with calcium activation is the NDH-2 of *Plasmodium falciparum* (pfNDH-2) [46]. Interestingly, the um03669, as well as the other three fungal sequences analyzed in Fig. 2, lack the two essential negative residues and the hydroxylated amino acid residue required for calcium binding. These residues correspond to the *z* and *x* positions in the loop for the Ca^{2+} binding domain, defined by the X—Y-Z—Y–X–Z motif [47].

Cell growth in different media

To study the expression and role of the three rotenone-resistant dehydrogenases from *U. maydis*, growth curves were obtained under the following culture conditions: YPD, glucose minimal (Glc-mm), ethanol minimal (EtOH-mm), and lactate minimal (Lac-mm) media. When cells were cultured in YPD, Glc-mm, or EtOH-mm, the stationary phase was reached at about

24 h after inoculation (Fig. S1 and [26]). As shown in Fig. S2, the concentration of glucose in the culture medium was still high after 24 h of growth. In contrast, for cells grown with other gluconeogenic carbon sources such as Lact-mm, the stationary phase was reached at around 150 h (Fig. S1 and [26]). YPD was the best condition for cell growth, with the highest biomass production (8 g wet weight·L^{-1}) and a duplication time of 2.4 h. Ethanol was also a good carbon source for the generation of biomass in short times (duplication time of 3.2 h). With lactate, the duplication time was over 20 h (Fig. S1 and [26]).

Respiratory activities by permeabilized cells

Next, cells harvested at the exponential or stationary phases were permeabilized in the same Clark electrode chamber with digitonin at a final concentration of 0.03–0.2% (w/v), as described by Vercesi [27]. Oxygen consumption assays in permeabilized cells were performed with different substrates and inhibitors (Figs 3 and 4). Both NADH and NADPH were used to assess the participation of the alternative external NADH and NADPH dehydrogenases. Pyruvate–malate was used to evaluate the activity of the internal NADH dehydrogenase. In all cases in which the NDH-2 was studied, the experiments were carried out in the presence of 10 μM of rotenone. The concentration of rotenone used in the assay was sufficient to inhibit complex I but not the NDH-2 [36]. To evaluate other electron input sites in the respiratory chain of *U. maydis* mitochondria, ethanol, succinate, glycerol 3-phosphate, or lactate was used to assess the participation of each specific dehydrogenase in both growth phases. As can be seen in Figs 3 and 4, permeabilized cells showed external rotenone-resistant NADH and NADPH dehydrogenase activities in both the exponential and stationary phases, regardless the culture conditions. The internal NADH dehydrogenase activity was found in both growth phases with ethanol and lactate as carbon sources, but with glucose, this activity was mostly present in the exponential phase.

A **Dinucleotide fold I**

```
klNDI1      SASFTTTKLIENNADNKPNVVILGSGWGAISFLQHIDAK---KYNVSIVSP
klNDE1      PPPQIPQAATFANGSPRKTLVVLGTGWGSVSLLKHLDTS---LYNVIVVSP
klNDE2      ETLDAYDSEMKELTSYKPKLVVLGSGWASVGLLKNLNPG---DYDVTVVSP
scNde1      PSTQVPQSDTFPNGSKRKTLVILGSGWGSVSLLKNLDTT---LYNVVVVSP
scNde2      PPKQVPQSTAFANGLKKKELVLGTGWGAISLLKKLDTS---LYNVTVVSP
scNdi1      PTSFKTMKVIDPQHSDKPNVLILGSGWGAISFLKHIDTK---KYNVSIISP
um11333     ASAR------------KQRLVVLGTGWGGYAFLKSLSYASLRRFDVKVISP
um02164     PPDQLPQD------PSKKTIVVLGSGWGATSLLKNIDTE---EYNVVVISP
um03669     SYAEDEQDEISKKLANKERLVIVGGGWAAVGLLKSLDPE---KYNVTLISP
ncNdi1      LTARNFSTVKFNNKDKRERVVILGSGWAGYSFAKDLDPE---KYERIFISP
ncNde1      IFLDDDDSEEKKKHKEKPRLVILGGGWGSVALLKELNPD---DYHVTVVSP
ncNde2      PGPQVEPD------PSKKTLVVLGTGWGSVSLLKKLDTE---HYNVIVISP
NDB1_SOLTU  VESGKQVVEQNQPESKKKRVVVLGTGWGGTSFLKDVDIS---SYDVQVVSP
                                 .   . ..:* ** .  . .:.       :.   .:**
```
                                   LG-GWG
                          First glycine rich motif

B **Dinucleotide fold II**

```
klNDI1      LLTIVVVGGGPTGVETAGELQDYVDQDLKRFMP-SIAEEVQIHLVEALPNV
klNDE1      LLSEVVVGGGPTGVEFAAELQDYVDQDLSKWIP-EISKEIKVTLVEALPNI
klNDE2      LLSEVVCGGGPTGVEFAAEVFDLLNEDLPSMYPRILRQQLSVHVIQSRSNI
scNde1      LLSEVVVGGGPTGVEFAAELRDYVDQDLRKWMP-ELSKEIKVTLVEALPNI
scNde2      LLTEVVVGGGPTGVEFAAELQDYINQDLRKWMP-DLSKEMKVILIEALPNI
scNdi1      LLSIVVVGGGPTGVEAAGELQDYVHQDLRKFLP-ALAEEVQIHLVEALPIV
um11333     LLSEVVVGGGPTGSEFAAELHDLINDELSRLYP-NVCAYATVRLLDAGSTI
um02164     LLHMVVVGGGPTGIEYAAELRDFVESDLIRWYP-EVANKLRVTLVEALPNI
um03669     LLSEVVCGGGPTGVETAAEISDMINEDVFDYFPKVLRAQAQVHLIQSREHI
ncNdi1      LLHEAIVGGGPTGIEYASELHDLIHDDLSKMYP-DLLKFVRITVYDVSPKV
ncNde1      LLSEVVCGGGPTGVEFAAELFDLLNEDLTLHFPRLLRNEISVHLIQSRDHI
ncNde2      LLHMVVVGGGPTGVEFAGELQDFFEEDIKKLIP-DIADRFRVTLIEALPNV
NDB1_SOLTU  NLHEVIVGGGPTGVEFAAELHDYVYEDLVKIYP-SVKDFVKITVIQSGDHI
              *  .  . ****** *  * *.*:  *   . .::        *   :      : : :       :
```
                              VVVGGGPTG
                        Second glycine-rich motif

Fig. 1. Multiple alignment using 13 NDH-2 sequences. The first three sequences (klNDI1, klNDE1, klNDE2) correspond to *Kluyveromyces lactis* NDH-2. The next three (scNde1, scNde2, and scNdi1) are the *NDH-2 of Saccharomyces cerevisiae*. The following three sequences correspond to the three NDH-2 of *U. maydis* (um11333, um2164, and um3669). The next three sequences correspond to *Neurospora crassa* NDH-2 (ncNdi1, ncNde1, ncNde2). Finally, the last sequence corresponds to an NDH-2 of *Solanum tuberosum*. The alignment was performed using Clustall W2 (http://www.ebi.ac.uk/Tools/msa/clustalw2). Symbols: '*', the amino acid is conserved in all sequences; ':', the amino acid type is conserved; '.', the amino acid profile is preserved. In both panels, the glycine-rich motifs are highlighted with blue boxes. Hydrophobic amino acids are colored yellow, residues with negative charge in red, residues with a hydroxyl group in purple, and proline and cysteine in white. Shaded in gray inside the third blue box are placed the amino acid with negative charge (D or E) or with a carboxamide group (N or Q) proposed by Desplats [37] as acidic or no acidic sequences that discriminate the activity of NADH or NADPH dehydrogenase. The um03669 sequence is colored green.

In general, activities were higher in the exponential phase than in the stationary phase for all the culture conditions (Fig. 3). Although oxygen consumption was higher with NADH than with NADPH, both activities were within the same order of magnitude. All the pathways feeding the electron transport chain were active in the exponential phase, independently of the culture media. On the other hand, in the stationary

```
                    Incoming helix                              Exiting helix      Linker
                                         Ca²⁺-Binding loop
                                         X  Y  Z      -Y -X -Z
calcyclin     --PLDQAIGLLVAIFHKY         SGREGDKH     TL  SKKE—      LKELIQKEL      TIGSKLQ----
calmodulin    ----EEQIAEFKEAFSLF         DK—DGDG      TI  TTKE-----LGTVMRS         LGQNPT----
myosin_RLC    ----QKQIQEMKEAFSMI         DV—DRDG      FV  SKED-----IKAISEQ         LGRAPD----
myosin_ELC    -----DEIDDLKDVFELF         DFWD-GRDG    AV  DAFK-----LGDVCRC         LGINPR----
klNde2        SNEIITDEDIKHLSLSYN         EIIDIAKQ     VA  RRHP-----QTREHLIH        LEDDLP---
um03669       ----DRYDKDKDGKLSY          SEFETFAQ     AI  RRKFP-----IASKHFIK       LREVFDQ--
ncNdi1        ----VLGDAAVIEKLSY          SEFETFAQ     AI  RRKFP-----IASKHFIK       LREVFD---
ncNde1        AVGDCAVAGPESLELHF          SDWRDVAQQ    IK  KRFP-----QATAHLKR        LDKLFEE--
NDB1_SOLTU    ----KAADKDDSGTLSI          EEFRDVLED    II  IR-YPQVDLYLKNKHL         LEAKDLFRDSE
                         :                  .                .
```

Fig. 2. Multiple sequence alignment for the calcium binding domain (CBD). The amino acids involved in Ca²⁺-binding are in bold type and highlighted; those that contribute with the main-chain carbonyl oxygen are shaded in gray, as proposed by Graberek [46]. Hydrophobic amino acids are colored in yellow, the residues with a positive charge in blue, with a negative charge in red, and with a hydroxyl group in purple. Calcium binding has been experimentally determined in the four mammalian proteins (calcyclin, calmodulin, myosin_RLC, and myosin_ELC); in addition, 4 fungal sequences (klNde2, um03669, ncNdi1, ncNde1) and the sequence of the plant *Solanum tuberosum* (NDB1_SOLTU) are shown.

phase there was a large decrease in oxygen consumption driven by pyruvate–malate, NADH, glycerol 3-phosphate, lactate, and ethanol. This was more evident in cells obtained from YPD and Glc-mm, in which some of the activities were undetectable. It is worth noting that oxygen consumption rates with NADH and ethanol as respiratory substrates were twofold higher in cells grown in nonglycolytic carbon sources (EtOH-mm and Lac-mm) in comparison with media containing glucose, and this observation occurred in both, the exponential and stationary phases. Ethanol was a good respiratory substrate, mostly in cells from the exponential phase of growth, and oxygen consumption was not altered by the addition of NAD$^+$ (Figs 3 and 4E), suggesting that the alcohol dehydrogenase is located in the mitochondrial matrix. In contrast to lactate, ethanol supported a rapid growth of the cells, resembling the growth kinetics obtained in the presence of glucose. This finding is interesting because there is no lactic or alcoholic fermentation in *U. maydis* yeast [34,36], but cells can consume very efficiently ethanol as a carbon source and as a respiratory substrate. The results also show that the expression of the alcohol, glycerol 3-phosphate, and lactate dehydrogenases was not specific for each culture condition. Thus, when cells were grown in ethanol, respiratory activities in permeabilized cells can be supported by lactate and glycerol 3-phosphate. It seems that when *U. maydis* yeasts are cultured in media with gluconeogenic carbon sources (ethanol and lactate) or under conditions of high energy demand (exponential phase), several pathways that feed the electron transport chain are expressed in mitochondria. However, we found that during the exponential phase,

the activity of some components (external NADH-DH, G3P-DH, lactate-DH, and EtOH-DH) was lower in cells cultured in the presence of glucose (Fig. 3). This decrease was more evident during the stationary phase, in which the activities of the G3P-DH, lactate-DH, and EtOH-DH were insignificant in cells cultured in the presence of glucose (Fig. 3). It should be noted that the concentration of glucose in the culture medium is still high in the stationary phase (Fig. S2) [48].

Next, we studied the activity of the respiratory chain of *U. maydis* to sequential additions of different substrates. Regardless of the order of addition of saturating concentrations of either NADH or NADPH, there was no increase in the oxygen consumption upon the addition of the second substrate, for example, adding NADH after NADPH did not increase the respiratory activity (Fig. 4A). This result suggests that both substrates interact with the same NDH-2 enzymes. In contrast, once the saturation with NADH or NADPH was reached, a subsequent addition of succinate, pyruvate–malate, or glycerol 3-phosphate increased the rate of oxygen consumption (Fig. 4B). Figure 4C shows that NADPH dehydrogenase activity did not respond to high concentrations of calcium, as occurs in other fungal systems such as *N. crassa* and some plants [41,44]. As both the mRNA and the protein with the calcium binding domain (um03669) were synthesized in the four culture conditions, the lack of an effect of calcium on the respiratory activity of permeabilized cells is in agreement with the absence of critical residues in the putative calcium binding domain of this protein. The experiment displayed in Fig. 4D suggests the presence of an internal NDH-2, insensitive to rotenone but sensitive to flavone.
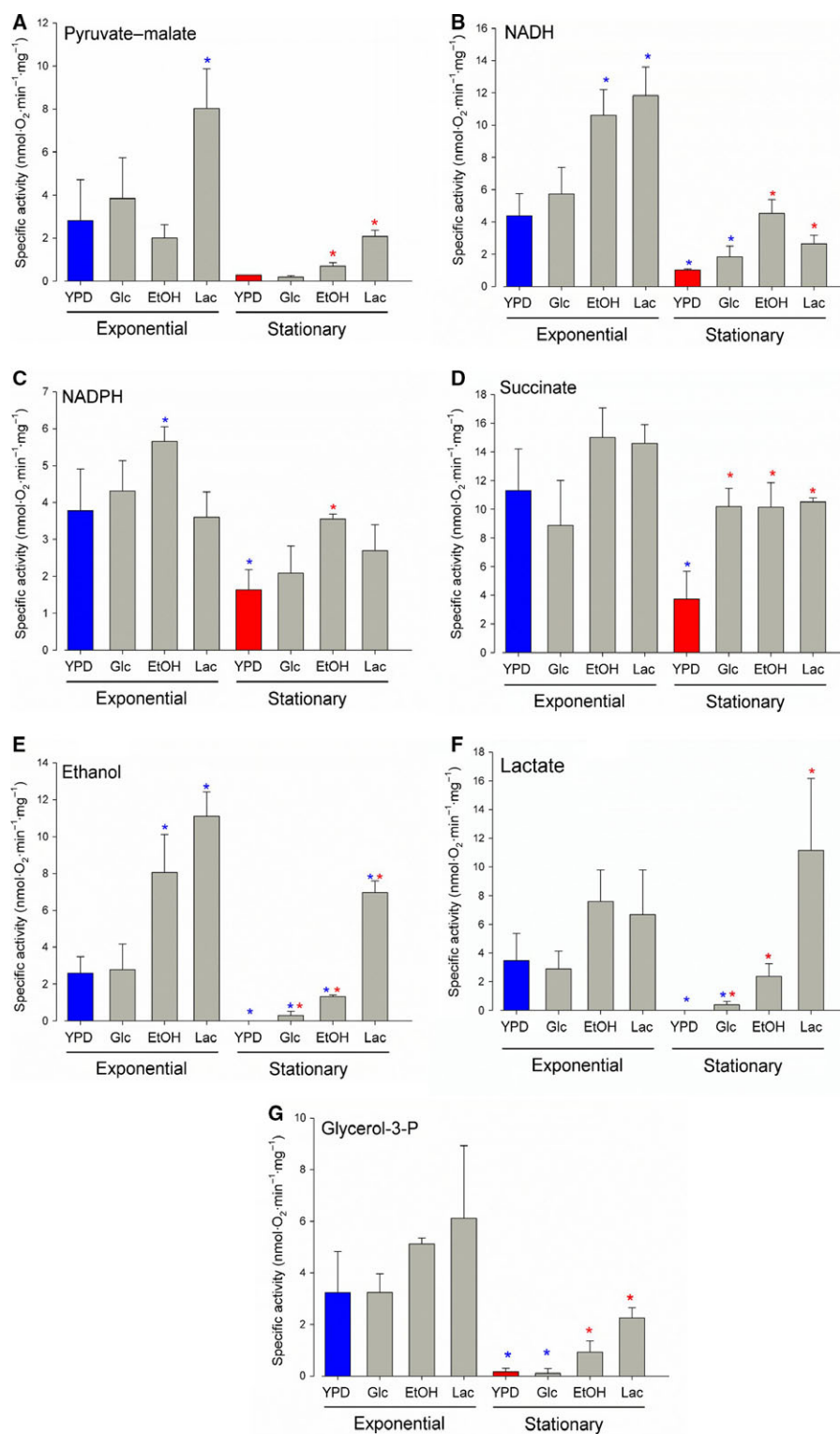
Fig. 3. Oxygen consumption by permeabilized cells. Cells were permeabilized with digitonin inside the oxymeter chamber following standardized methods proposed by Robles-Martínez [48]. After permeabilization, different respiratory substrates were used to evaluate the rate of oxygen consumption. (A) 5 mM pyruvate-malate, (B) 1 mM NADH, (C) 1 mM NADPH, (D) 7 mM succinate, (E) 130 mM ethanol, (F) 15 μM lactate and (G) 1 mM glycerol-3-phosphate. Data represent the average and standard deviation of three independent experiments. Blue asterisks on the bars indicate a significant difference with respect to the exponential-YPD condition. Within the stationary phase, red asterisks indicate a significant difference taking as control the stationary-YPD condition. A two-way ANOVA was used for the analysis with a $P < 0.05$.
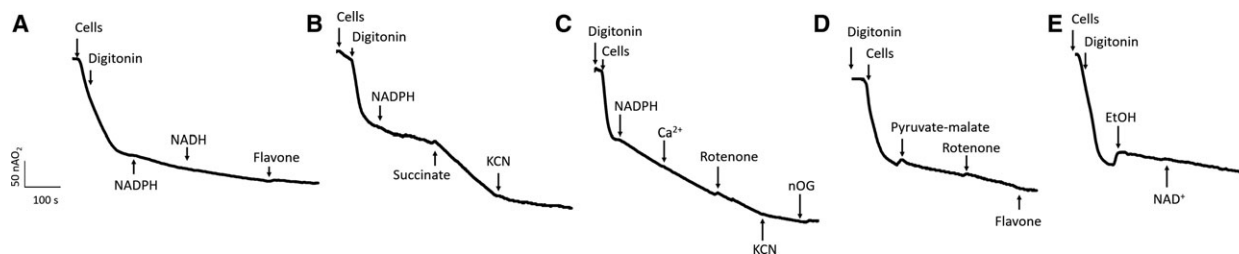
Fig. 4. Time courses of oxygen consumption by permeabilized *U. maydis* cells harvested at the exponential phase. Cells were permeabilized with digitonin inside the oxymeter chamber following standardized methods proposed by Robles-Martínez [48]. After permeabilization, oxygen consumption was stimulated by the addition of the indicated substrates. (A) NADPH, NADH and flavone. (B) NADPH, succinate, and KCN. (C) NADPH plus calcium, followed by rotenone, KCN and nOG. (D) To discriminate between complex I and the internal NDH-2 activities, pyruvate-malate was used as substrate, and rotenone plus flavone to inhibit the respiratory chain activity. (E) Ethanol plus NAD^+. For permeabilization of cells, digitonin at 0.03% (v/v) was used. The concentration of substrates was: 10 mM succinate, 130 mM ethanol, 1 mM NADH, 1 mM NADPH, and 5 mM of both pyruvate and malate. Inhibitors were used at the following concentrations: 10 μM rotenone, 47 μM flavone, 1 mM potassium cyanide (KCN), 1 μM *n*-octylgalate (nOG). Calcium was used at a concentration of 1.2 mM, and NAD^+ at 1 mM.

RNA and protein expression

Expression of the three *U. maydis* NADH dehydrogenases was analyzed by RT-PCR in cells harvested at the stationary phase of growth. For normalization, the actin mRNA was used as reference [49]. Figure 5 shows similar levels of expression for the three RNA transcripts in cells cultured under different conditions. Proteomic analysis further revealed that only the NADH dehydrogenases um02164 and um03669 were associated with mitochondria of *U. maydis* cells cultured in EtOH-mm, Lac-mm, and YPD culture media and harvested at the exponential phase of growth (Table 2), while peptides of um11333 were not detected in mitochondria. Taken together, these results suggest that in *U. maydis* a posttranscriptional regulation may exist that allows the differential translation of certain mRNA. In addition, due to the important role of these enzymes in the intermediary metabolism, regulation by covalent modifications like phosphorylation–dephosphorylation should be considered. In this sense, there are several putative phosphorylation sites in the amino acid sequences of the three NDH-2 from *U. maydis* (data not shown). In support of this suggestion, phosphorylation of scNDI1 and scNDE1 has been reported [50,51].

The role of the alternative NAD(P)H dehydrogenases in *Ustilago maydis*

To place these dehydrogenases in the metabolic context of the cells, information about the presence of some proteins belonging to central metabolic pathways under the three culture conditions (YPD, EtOH-mm, and Lac-mm) was obtained through proteomic analysis. In general, the expression of the enzymes that
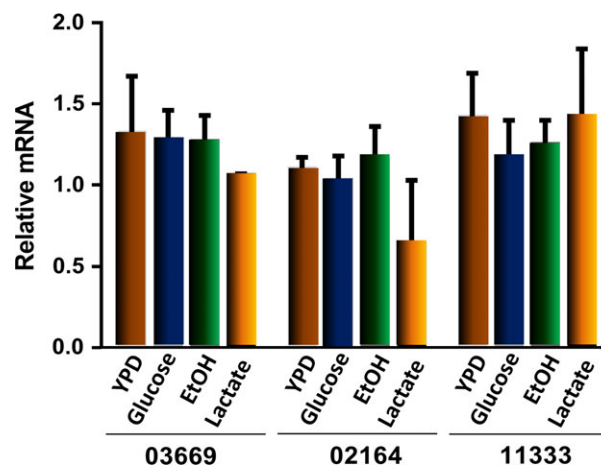

Fig. 5. Reverse transcription-polymerase chain reaction of the NDH-2s transcripts in *Ustilago maydis*. Cells grown under different conditions and harvested at the exponential phase were disrupted to obtain total RNA. Using the primers described in Table 1, RT-PCR was carried out to evaluate the levels of each transcript using the actin transcript for normalization. Data represent the average of three independent experiments.

belong to carbon metabolism was not associated with the culture conditions of the cells. For example, with the gluconeogenic substrates ethanol and lactate, the three classic regulatory glycolytic enzymes, hexokinase, phosphofructokinase-1, and pyruvate kinase were expressed (Fig. 6). During the exponential phase, there was no difference between the YPD and Glc-mm in the activities of the three enzymes, but with ethanol as the carbon source, there was a large decrease in their activities. Similarly, in EtOH-mm and Lac-mm, there was a decrease in the activities of PFK-1 and PK.

Table 2. Representative enzymes of some metabolic pathways found in cells cultured under different culture conditions. The samples were sent to the research laboratory in Arizona, USA, as described under the materials and methods. The numbers represent a weighted value of the abundance of each protein under each condition. 6-P-gluconate dehydrogenase, 6 phosphogluconate dehydrogenase; Aox, alternative oxidase; FBPase-1, fructose bisphosphatase 1; G3PDH, glyceraldehyde 3 phosphate dehydrogenase; Glc-6-P dehydrogenase, glucose-6-phosphate dehydrogenase; Glycerol-3-P dehydrogenase, glycerol-3-phosphate dehydrogenase; GPI, glucose 6 phosphate isomerase; ND, no determined; ND2, alternative NADH dehydrogenase 2; PEP-CK, phosphoenolpyruvate carboxykinase; PGK, phosphoglycerate kinase; PK, pyruvate kinase; TPI, triose phosphate isomerase.

Enzyme	Accession number	YPD	EtOH-mm	Lac-mm
Glycolysis				
GPI	A0A0D1DUK2	5	12	5
Aldolase	A0A0D1E8V6	6	12	12
TPI	A0A0D1DYK6	ND	9	6
G3P dehydrogenase	A0A0D1CU24	7	13	19
PGK	A0A0D1DSH4	12	13	12
Enolase	A0A0D1E2E4	11	13	9
PK	A0A0D1E735	14	22	15
Gluconeogenesis				
FBPase-1	A0A0D1C717	ND	8	ND
PEP-CK	A0A0D1E2J3	ND	32	25
Phosphate pentose pathway				
Glc-6-P dehydrogenase	A0A0D1BZD5	5	4	ND
6-P-gluconate dehydrogenase	A0A0D1CRJ9	13	12	17
Transaldolase	A0A0D1DYQ2	3	5	6
Transketolase	A0A0D1CJR1	8	10	14
Krebs cycle				
Citrate synthase	A0A0D1CAY8	23	20	18
Aconitase	A0A0D1DXN8	28	26	38
Isocitrate dehydrogenase	A0A0D1E633	17	18	15
2-oxoglutarate dehydrogenase	A0A0D1CAI6	15	7	11
Succinyl-CoA synthase	A0A0D1E476	12	9	9
Succinate dehydrogenase	A0A0D1DVG5	16	41	43
Fumarase	A0A0D1E945	12	6	11
Malate dehydrogenase	A0A0D1BZ90	6	20	18
Respiratory complexes and ATP synthase				
Complex I	A0A0D1DQS4	15	26	33
Complex II	A0A0D1CDW6	16	41	43
Complex III	A0A0D1CAD4	24	28	26
Complex IV	A0A0D1DRD6	13	14	11
Complex V	A0A0D1E227	45	62	57
Respiratory alternative elements				
Lactate dehydrogenase	A0A0D1E9U3	ND	7	27
ND2 um02164	A0A0D1E082	7	18	24
ND2 um03669	A0A0D1DV23	24	7	16
Glycerol-3P dehydrogenase	A0A0D1CVJ0	15	10	21
Aox	A0A0D1C7C6	ND	11	3

When cells entered the stationary phase, the activities of the three enzymes in YPD increased twice, but this was not observed in Glc-mm. Regarding the PFK-1 and PK, their activities were lower in EtOH-mm and Lac-mm than in YPD or even Glc-mm. Interestingly, the activity of the hexokinase is high in all conditions, with the exception of ethanol in the exponential phase. In short, it can be said that with the exception of the HK, the activities of the two glycolytic enzymes were smaller in cell growing with the two gluconeogenic substrates, ethanol and lactate. Given the relative high activity of regulatory glycolytic enzymes in cells growing in gluconeogenic media (Fig. 6), it is expected that some type of control mechanism occurs to avoid energetically expensive futile cycles. Table 2 shows that enzymes from glycolysis, Krebs cycle, pentose phosphate pathway, and gluconeogenesis were present in cells regardless of the carbon source (glucose, ethanol, or lactate). The mitochondrial flavoenzyme lactate dehydrogenase was expressed mainly in the presence of
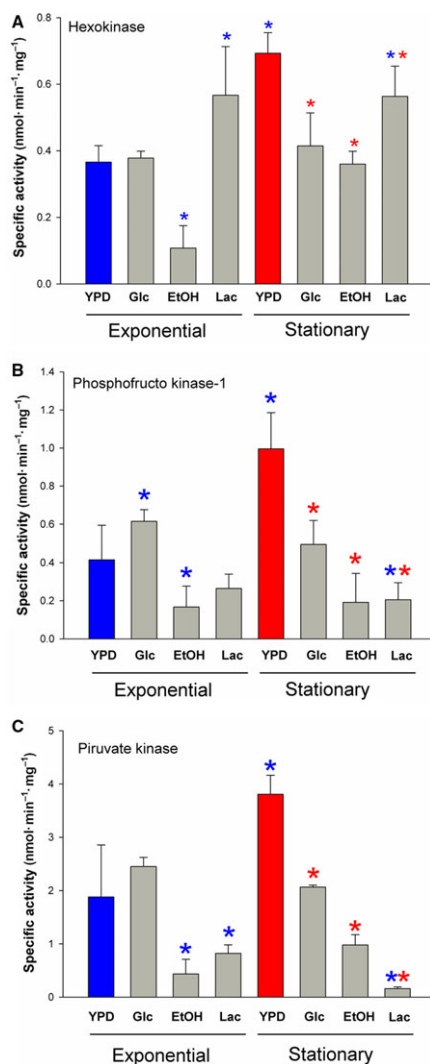
Fig. 6. Specific activities of hexokinase, phosphofructokinase-1, and pyruvate kinase in *U. maydis* cell extracts. Enzyme activity was determined as described in Saavedra *et al.* [34]. Data represent the average and standard deviation of five independent experiments. (A) For hexokinase, the activity was measured in a reaction mixture containing 5 mm $MgCl_2$, 1 mm NADPH, 5 mm glucose, 2 U G6PDH, 13–68 mg of cytosolic extract. The reaction was started by the addition of 3 mm ATP. (B) For the phosphofructokinase-1, the reaction mixture contained 5 mm $MgCl_2$, 1 mm EDTA, 0.15 mm NADH, 3 mm ATP, 0.5–1 U aldolase, 3 U Gly3PDH – 4.5 U triose phosphate isomerase (Roche) and 30–400 mg of cytosolic extract. The reaction was started by the addition of 2.5 mm fructose 6 phosphate. (C) Pyruvate kinase was assayed in a reaction mixture containing 10 mm $MgCl_2$, 0.15 mm NADH, 1 mm phosphoenopyruvate, 2.5 U lactate dehydrogenase, 13–90 mg of cytosolic extract. The reaction was started with 3 mm ADP. Blue asterisks on the bars indicate a significant difference with respect to the exponential-YPD condition. Within the stationary phase, red asterisks indicate a significant difference taking as control the stationary-YPD condition. A two-way ANOVA was used for the analysis with a $P < 0.05$.

lactate, and to a lesser extent with ethanol, but not in YPD. In contrast, the mitochondrial glycerol 3-phosphate dehydrogenase and the two alternative NADH dehydrogenases were expressed under all the conditions.

Activity of the mitochondrial external NADH dehydrogenase makes sense in the context of *U. maydis* metabolism. As this organism is fully respiratory, these enzymes are essential for the continuous operation of glycolysis and other metabolic routes that depend on the availability of NAD^+. In contrast, the role of the NADPH dehydrogenase activity is more difficult to explain, because in many anabolic pathways, NADPH is used as substrate. In a previous work, we found that the activities of the enzymes in the oxidative phase of the phosphate pentose pathway [52] are more active than the glycolytic enzymes reported by Saavedra *et al.* [34]. Thus, it is possible that the NADPH dehydrogenase activity in mitochondria allows the rapid and efficient oxidation of NADPH produced in the pentose pathway.

Ustilago maydis has been extensively used for years as a model to study the participation of several signal transduction pathways in the yeast-mycelium transition and pathogenicity [53,54], or more recently the introduction of this microorganism for biotechnological applications [55,56]. In sharp contrast with this vast information, the mechanisms underlying the metabolic changes described in this work are still unknown. Cloning and expression of the three NADH dehydrogenases will allow the determination of their specificities and kinetic parameters, and the evaluation of the effect of calcium on the activity of the um03669 enzyme.

Acknowledgements

Author contributions

AP conceptualized and coordinated the research project, provided funding to support the research, and reviewed and edited the manuscript. JPP conceptualized and coordinated the research project, analyzed the data, provided funding to support the research, and reviewed and edited the manuscript. GGS conceptualized the research project, provided funding to support the research, and reviewed the manuscript. GMO conceptualized, coordinated, and developed the research project; performed the bioinformatics analyses, PCR and protein data analyses, and oxygen consumption assays; and wrote the original draft. DMM isolated mitochondria, performed SDS/PAGE with mitochondrial samples, analyzed the data, and reviewed the manuscript. CCM performed PCR analyses and oxygen consumption assays analysis. JCV determined the glycolytic enzyme-specific activities and analyzed the data. LRA performed yeast growth and glucose determination, and performed SDS/PAGE with mitochondrial samples. HVM isolated mitochondria, protein analysis, and oxygen consumption assays.

References

1 Rustin P and Jacobs HT (2009) Respiratory chain alternative enzymes as tools to better understand and counteract respiratory chain deficiencies in human cells and animals. *Physiol Plant* **137**, 362–370.

2 De Vries S and Grivell LA (1988) Purification and characterization of a rotenone-insensitive NADH:Q6 oxidoreductase from mitochondria of *Saccharomyces cerevisiae*. *Eur J Biochem* **176**, 377–384.

3 Rasmusson AG, Geisler DA and Moller IM (2008) The multiplicity of dehydrogenases in the electron transport chain of plant mitochondria. *Mitochondrion* **8**, 47–60.

4 De Vries S, Van Witzenburg R, Grivell LA and Marres CA (1992) Primary structure and import pathway of the rotenone-insensitive NADH-ubiquinone oxidoreductase of mitochondria from *Saccharomyces cerevisiae*. *Eur J Biochem* **203**, 587–592.

5 Melo AM, Bandeiras TM and Teixeira M (2004) New insights into type II NAD(P)H:quinone oxidoreductases. *Microbiol Mol Biol Rev* **68**, 603–616.

6 Velazquez I and Pardo JP (2001) Kinetic characterization of the rotenone-insensitive internal NADH: ubiquinone oxidoreductase of mitochondria from *Saccharomyces cerevisiae*. *Arch Biochem Biophys* **389**, 7–14.

7 Yamashita T, Nakamaru-Ogiso E, Miyoshi H, Matsuno-Yagi A and Yagi T (2007) Roles of bound quinone in the single subunit NADH-quinone oxidoreductase (Ndi1) from *Saccharomyces cerevisiae*. *J Biol Chem* **282**, 6012–6020.

8 Kerscher SJ (2000) Diversity and origin of alternative NADH:ubiquinone oxidoreductases. *Biochim Biophys Acta* **1459**, 274–283.

9 Matus-Ortega MG, Salmerón-Santiago KG, Flores-Herrera O, Guerra-Sánchez G, Martínez F, Rendón JL and Pardo JP (2011) The alternative NADH dehydrogenase is present in mitochondria of some animal taxa. *Comp Biochem Physiol Part D Genomics Proteomics* **6**, 256–263.

10 Iwata M, Lee Y, Yamashita T, Yagi T, Iwata S, Cameron AD and Maher MJ (2012) The structure of the yeast NADH dehydrogenase (Ndi1) reveals overlapping binding sites for water- and lipid-soluble substrates. *Proc Natl Acad Sci USA* **109** (38), 15247–15252.

11 Feng Y, Li W, Li J, Wang J, Ge J, Xu D, Liu Y, Wu K, Zeng Q, Wu JW *et al.* (2012) Structural insight into the type-II mitochondrial NADH dehydrogenases. *Nature* **491**, 478–482.

12 Heikal A, Nakatani Y, Dunn E, Weimar MR, Day CL, Baker EN, Lott JS, Sazanov LA and Cook GM (2014) Structure of the bacterial type II NADH dehydrogenase: a monotopic membrane protein with an essential role in energy generation. *Mol Microbiol* **91**, 950–964.

13 Small WC and McAlister-Henn L (1998) Identification of a cytosolically directed NADH dehydrogenase in mitochondria of *Saccharomyces cerevisiae*. *J Bacteriol* **180**, 4051–4055.

14 Luttik MA, Overkamp KM, Kötter P, de Vries S, van Dijken JP and Pronk JT (1998) The *Saccharomyces cerevisiae* NDE1 and NDE2 genes encode separate mitochondrial NADH dehydrogenases catalyzing the oxidation of cytosolic NADH. *J Biol Chem* **273**, 24529–24534.

15 Grandier-Vazeille X, Bathany K, Chaignepain S, Camougrand N, Manon S and Schmitter JM (2001) Yeast mitochondrial dehydrogenases are associated in a supramolecular complex. *Biochemistry* **40**, 9758–9769.

16 Matus-Ortega MG, Cárdenas-Monroy CA, Flores-Herrera O, Mendoza-Hernández G, Miranda M, González-Pedrajo B, Vázquez-Meza H and Pardo JP (2015) New complexes containing the internal alternative NADH dehydrogenase (Ndi1) in mitochondria of *Saccharomyces cerevisiae*. *Yeast* **32**, 629–641.

17 Eubel H, Jansch L and Braun HP (2003) New insights into the respiratory chain of plant mitochondria:

supercomplexes and a unique composition of complex II. *Plant Physiol* **133**, 274–286.

18 Dudkina NV, Heinemeyer J, Sunderhaus S, Boekema EJ and Braun HP (2006) Respiratory chain supercomplexes in the plant mitochondrial membrane. *Trends Plant Sci* **11**, 232–240.

19 Ramirez-Aguilar SJ, Keuthe M, Rocha M, Fedyaev VV, Kramp K, Gupta KJ, Rasmusson AG, Schulze WX and van Dongen JT (2011) The composition of plant mitochondrial supercomplexes changes with oxygen availability. *J Biol Chem* **286**, 43045–43053.

20 Lin SS, Gross U and Bohne W (2009) Type II NADH dehydrogenase inhibitor 1-hydroxy-2-dodecyl-4(1H) quinolone leads to collapse of mitochondrial inner-membrane potential and ATP depletion in *Toxoplasma gondii*. *Eukaryot Cell* **8**, 877–887.

21 Horne JT, Hollomon DW and Wood PM (2001) Fungal respiration: a fusion of standard and alternative components. *Biochim Biophys Acta* **1504**, 179–195.

22 Bald D and Koul A (2010) Respiratory ATP synthesis: the new generation of mycobacterial drug targets. *FEMS Microbiol Lett* **308**, 1–7.

23 Bai Y, Hájek P, Chomyn A, Chan E, Seo BB, Matsuno-Yagi A, Yagi T and Attardi G (2001) Lack of complex I activity in human cells carrying a mutation in MtDNA-encoded ND4 subunit is corrected by the *Saccharomyces cerevisiae* NADH-quinone oxidoreductase (NDI1) gene. *J Biol Chem* **276**, 38808–38813.

24 Seo BB, Marella M, Yagi T and Matsuno-Yagi A (2006) The single subunit NADH dehydrogenase reduces generation of reactive oxygen species from complex I. *FEBS Lett* **580**, 6105–6108.

25 Hur JH, Bahadorani S, Graniel J, Koehler CL, Ulgherait M, Rera M, Jones DL and Walker DW (2013) Increased longevity mediated by yeast NDI1 expression in Drosophila intestinal stem and progenitor cells. *Aging (Albany NY)* **5**, 662–681.

26 Cárdenas-Monroy CA, Pohlmann T, Piñón-Zárate G, Matus-Ortega G, Guerra G, Feldbrügge M and Pardo JP (2017) The mitochondrial alternative oxidase Aox1 is needed to cope with respiratory stress but dispensable for pathogenic development in *Ustilago maydis*. *PLoS ONE* **12**, e0173389. https://doi.org/10.1371/journal.pone.0173389

27 Vercesi AE, Bernardes CF, Hoffmann ME, Gadelha FR and Docampo R (1991) Digitonin permeabilization does not affect mitochondrial function and allows the determination of the mitochondrial membrane potential of *Trypanosoma cruzi* in situ. *J Biol Chem* **266**, 14431–14434.

28 Altschul SF, Madden TL, Schäffer AA, Zhang J, Zhang Z, Miller W and Lipman DJ (1997) Gapped BLAST and PSI-BLAST: a new generation of protein database search programs. *Nucleic Acids Res* **25**, 3389–3402.

29 Thompson JD, Higgins DG and Gibson TJ (1994) CLUSTAL W: improving the sensitivity of progressive multiple sequence alignment through sequence weighting, position-specific gap penalties and weight matrix choice. *Nucleic Acids Res* **22**, 4673–4680.

30 Claros MG (1995) MitoProt, a Macintosh application for studying mitochondrial proteins. *Comput Appl Biosci* **11**: 441–447.

31 Holliday R (1974) *Ustilago maydis. Handbook of Genetics*. Plenum, New York, NY, **1**, 575–595.

32 Robles-Martínez L, Guerra-Sánchez MG, Flores-Herrera O, Hernández-Lauzardo AN, Velázquez-Del Valle MG and Pardo JP (2013) The mitochondrial respiratory chain of Rhizopus stolonifer (Ehrenb.:Fr.) Vuill. *Arch Microbiol* **195**, 51–61.

33 Sierra-Campos E, Velázquez I, Matuz-Mares D, Villavicencio-Queijeiro A and Pardo JP (2009) *Functional properties of the Ustilago maydis alternative oxidase under oxidative stress conditions. Mitochondrion* **2**, 96–102.

34 Saavedra E, Ramos-Casillas LE, Marín-Hernández A, Moreno-Sánchez R and Guerra-Sánchez G (2008) Glycolysis in *Ustilago maydis*. *Federat Europ Microbiol Societ* **8**, 1313–1323.

35 Laemmli UK (1970) Cleavage of structural proteins during the assembly of the head of bacteriophage T4. *Nature* **227**, 5259.

36 Juarez O, Guerra G, Martínez F and Pardo JP (2004) The mitochondrial respiratory chain of *Ustilago maydis*. *Biochim Biophys Acta* **1658**, 244–251.

37 Desplats C, Beyly A, Cuine S, Bernard L, Cournac L and Peltier G (2007) Modification of substrate specificity in single point mutants of *Agrobacterium tumefaciens* type II NADH dehydrogenase. *FEBS Lett* **581**, 4017–4022.

38 Blaza JN, Bridges HR, Dunn EA, Heikal A, Cook GM, Nakatani Y and Hirst J (2017) The mechanism of catalysis by type-II NADH:quinone oxidoreductases. *Sci Rep* **7**, 40615, https://doi.org/10.1038/srep40165

39 Meng-Shu H and Rasmusson AG (2016) The evolution of substrate specificity-associated residues and Ca2+-binding motifs in EF-hand-containing type II NAD(P) H dehydrogenases. *Physiol Plant* **157**, 338–351.

40 Matus-Ortega MG, Cárdenas-Monroy CA, Araiza-Villanueva M, Vázquez-Carrada M, Vázquez-Meza H, Matuz-Mares D and Guerra-Sánchez G, Peña-Díaz, Antonio y Pardo-Vázquez Juan Pablo (2017) *The alternative NADH dehydrogenases in fungi, new metabolic roles and its evolutionary history*. Memoria del 44° Taller de Actualización Bioquímica, Facultad de Medicina; UNAM http://tab.facmed.unam.mx/mensaje-bioquimica-2017.html

41 Melo AM, Duarte M, Møller IM, Prokisch H, Dolan PL, Pinto L, Nelson MA and Videira A (2001) The external calcium-dependent NADPH dehydrogenase

from *Neurospora crassa* mitochondria. *J Biol Chem* **276**, 3947–3951.

42 Carneiro P, Duarte M and Videira A (2004) The main external alternative NAD(P)H dehydrogenase of *Neurospora crassa* mitochondria. *Biochim Biophys Acta* **1608**, 45–52.

43 Tarrio N, Becerra M, Cerdán ME and González Siso MI (2006) Reoxidation of cytosolic NADPH in *Kluyveromyces lactis. FEMS Yeast Res* **6**, 371–380.

44 Hao MS, Jensen AM, Boquist AS, Liu YJ and Rasmusson AG (2015) The Ca2+-Regulation of the mitochondrial external NADPH dehydrogenase in plants is controlled by cytosolic pH. *PLoS ONE* **10**, 0139224.

45 Tarrio N, Cerdán ME and González Siso MI (2006) Characterization of the second external alternative dehydrogenase from mitochondria of the respiratory yeast *Kluyveromyces lactis. BBA* **1757**, 1476–1484.

46 Yang Y, Yu Li X, Li J, Wu Y, Yu J, Ge J, Huang Z, Jiang J, Rao Y and Yang M (2017) Target elucidation by cocrystal structures of NADH-ubiquinone oxidoreductase of *Plasmodium falciparum* (PfNDH2) with small molecule to eliminate drug-resistant malaria. *J Med Chem* **60**, 1994–2005.

47 Grabarek Z (2006) Structural basis for diversity of the EF-hand calcium-binding proteins. *J Mol Biol* **359**, 509–525.

48 Matus Ortega MG (2007) Caracterización cinética de la H$^+$-ATPasa de la levadura de *U. maydis* cultivada en medio mínimo y de YPD. *UNAM-Tesis* **1**, 56.

49 Robles-Martínez L, Pardo Juan Pablo, Tavis Manuel Miranda, Mendez L, Matus-Ortega Macario Genaro, Mendoza-Hernández Guillermo and Guerra-Sánchez Guadalupe (2013) The basidiomycete *Ustilago maydis* has two plasma membrane H+-ATPases related to fungi and plants. *J Bioenerg Biomembr* **45**, 477–490.

50 Reinders J, Wagner K, Zahedit R, Stojanovski D, Eyrich B, Laan M, Rehling P, Sickmann A, Pfanner N and Meisinger C (2007) Profiling phosphoproteins of yeast mitochondria reveals a role of phosphorylation in assembly of ATP synthase. *MCP* **6**, 1896–1906.

51 Renvoisé M, Bonhomme L, Davanture M, Valot B, Zivy M and Lemaire C (2014) Quantitative variations of the mitochondrial proteome and phosphoproteome during fermentative and respiratory growth in *Saccharomyces cerevisiae. J Proteomics* **106**, 140–150.

52 Romero-Aguilar L, Montero-Lomelí M, Luqueño-Bocardo OI, Juárez-Oropeza MA and Guerra-Sánchez G (2017) Lipid droplets accumulation and other biochemical changes induced in the fungal pathogen *Ustilago maydis* under nitrogen-starvation. *Arch Microbiol* **199**, 1195–1209.

53 Dean R, Van Kan JA, Pretorius ZA, Hammond-Kosack KE, Di Pietro A, Spanu PD, Rudd JJ, Dickman M, Kahmann R, Ellis J *et al.* (2012) The Top 10 fungal pathogens in molecular plant pathology. *Mol Plant Pathol* **13**, 414–430.

54 Vollmeister E, Schipper K, Baumann S, Haag C, Pohlmann T, Stock J and Feldbrügge M (2012) Fungal development of the plant pathogen *Ustilago maydis. FEMS Microbiol Rev* **6**, 59–77.

55 Terfrüchte M, Reindl M, Jankowski S, Sarkari P, Feldbrügge M and Schipper K (2017) Applying unconventional secretion in *Ustilago maydis* for the export of functional nanobodies. *Int J Mol Sci.* **18**, E937. https://doi.org/10.3390/ijms18050937

56 Feldbrügge M, Kellner R and Schipper K (2013) The biotechnological use and potential of plant pathogenic smut fungi. *Appl Microbiol Biotechnol* **97**, 3253–3265.

Supporting information

Additional supporting information may be found online in the Supporting Information section at the end of the article.

Fig. S1. *Ustilago maydis* growth curves in different culture media. Panel A shows the growth of *U. maydis* when the carbon source was glucose or ethanol. Panel B shows the growth in media with lactate as the carbon source. Tables show the growth rate constants (k) and duplication times (g).

Fig. S2. *Ustilago maydis* growth in YPD medium. Yeast growth was followed by absorbance at 600 nm. Simultaneously, the residual concentration of glucose in the culture medium was determined using a kit based on the glucose oxidase activity (Spinreact ®). Standard deviations for each point were obtained from three independent experiments.